Title
Compression Response of Sedimented Unsaturated Soils

Journal
Journal of Geotechnical and Geoenvironmental Engineering, 148(12)

ISSN
1090-0241

Authors
Behbehani, F
McCartney, JS

Publication Date
2022-12-01

DOI
10.1061/(asce)gt.1943-5606.0002931

Peer reviewed

COMPRESSION RESPONSE OF SEDIMENTED UNSATURATED SOILS

By F. Behbehani [1] and J.S. McCartney, Ph.D., P.E., F.ASCE[2]

ABSTRACT

This paper presents an experimental study on the hydro-mechanical behavior of unsaturated sedimented soil to understand the impacts of suction on the apparent yield stress and gain insight into the differences in behavior from compacted soils. A large-strain oedometer was developed for use in a triaxial cell that permits initial sedimentation of soils from a slurry under backpressure, suction control using the axis translation technique, and mechanical loading to characterize the compression curve. A flow pump was used to control the pore water pressure at the base of the soil specimen and to track water flow during suction application and mechanical loading. After initial consolidation of saturated soil specimens from a slurry, the specimens were unloaded, different suction values were applied, then the axial stress was increased to 11 MPa at a constant strain rate. An increase in apparent yield stress with suction was observed, and the compression curves for higher suctions diverged without reaching pressurized saturation in the applied stress range. When compared with compression curves for the same soil compacted dry of optimum presented in previous studies, the sedimented soil had a greater yield stress at saturated conditions but a similar increase in yield stress with suction. Sedimented soils also experienced smaller changes in void ratio with applied net stress and a higher air entry suction value compared to compacted soils, reflecting a more compact soil structure. Suction was found to have a greater impact on yield stress than suction stress for both sedimented and compacted soils.

[1] Assistant Professor, Department of Civil Engineering, College of Engineering and Petroleum, Kuwait University Al-Shadadiya, Kuwait, Email: fatemah.behbehani@ku.edu.kw
[2] Professor and Department Chair, Department of Structural Engineering, University of California San Diego, La Jolla, CA 92093-0085; Email: mccartney@ucsd.edu

INTRODUCTION

The compression response of unsaturated soils due to changes in net normal stress or suction has important implications on the performance of fill-type geotechnical structures involving compacted soils, but also cut-type geotechnical structures involving naturally sedimented soils. However, most previous studies on the compression response of unsaturated soils focused on the hydro-mechanical behavior of compacted soils (e.g., Wheeler & Sivakumar 1995; Sharma 1998; Maâtouk et al. 1995; Rampino et al. 1999; Al-Mukhtar et al. 1999; Lloret et al. 2003; Cuisinier & Masrouri 2005; Jotisankasa et al. 2007; Thu et al. 2007; Uchaipichat & Khalili 2009; Coccia & McCartney 2016; Khosravi et al. 2016, 2018; Mun & McCartney 2017). It is well accepted from the results of these studies that an increase in suction will lead to an increase in apparent yield stress, a feature that has been incorporated into most constitutive models for unsaturated soils (e.g., Alonso et al. 1990; Wheeler & Sivakumar 1995; Cui et al. 1995; Bolzon et al. 1996; Gallipoli et al. 2003; Sheng et al. 2008). However, the soil structure induced by compaction may also affect the yield stress, especially for the case that specimens are compressed after being compacted to different gravimetric water contents (e.g., Mun & McCartney 2017) instead of the case when different suctions are imposed after compaction (e.g., Uchaipichat & Khalili 2009; Coccia & McCartney 2016; Khosravi et al. 2016, 2018) or when specimens are wetted or dried after compaction and the suction is monitored (Jotisankasa et al. 2007). Soil specimens compacted at gravimetric water contents on the dry side of optimum will have a flocculated structure due to the formation of aggregates of fine particles, while soil specimens compacted at gravimetric water contents wet of optimum will have a dispersed structure where particles are aligned (e.g., Mitchell et al. 1965; Ahmed et al. 1974, Delage et al. 1996). Soils with a flocculated structure have higher compressibility, permeability, and undrained shear strength than soils with a dispersed structure

(Mitchell et al. 1965). Further, soils with a flocculated structure have stable intra-aggregate pores that are not affected by compaction but have inter-aggregate pores that may collapse during wetting (Tarantino & de Col 2008; Tarantino 2010; Gao et al. 2016).

Sedimentation of soil specimens from a slurry may lead to a different soil structure (or fabric) than induced by compaction, potentially affecting the yielding behavior of the soil when compressed in unsaturated conditions. Only a limited number of experimental studies have been performed on the volume change of unsaturated soil specimens sedimented from a slurry due to changes in suction (Fleureau et al. 1993) or changes in net stress (Jennings & Burland 1962; Cunningham et al. 2003; Geiser et al. 2006; Salager et al. 2008 Gao et al. 2016). However, in these studies, Fleureau et al. (1993) did not measure the compression curve after drying a slurry to a given suction so the changes in yield stress with suction were not detected, Jennings & Burland (1962) did not measure suction or track changes in degree of saturation, Cunningham et al. (2003) evaluated saturated and unsaturated specimens with different initial void ratios and did not observe a clear yield stress in the applied stress range of their compression tests, Geiser et al. (2006) and Salager et al. (2006) performed limited tests on unsaturated soils and did not make comparisons between compacted and sedimented soils, and although Gao et al. (2016) compared compression curves for compacted and sedimented soils they did not evaluate the impact of these soil preparation techniques on the yield stress versus suction relationship. A comparison between the compression responses of sedimented and compacted soils would be valuable in understanding the role of soil preparation technique and associated soil structure on the mechanisms of suction hardening in unsaturated soils. Accordingly, this study presents results from one-dimensional compression tests on saturated and unsaturated Bonny silt specimens sedimented from a slurry after which different matric suctions were applied to understand the impact of suction on the yield stress for this soil preparation technique, and to assess the hydro-mechanical response of the soil during compression including changes in degree of saturation and the suction stress at yielding. Bonny silt was selected for this study as data is available in the literature for its compression response in compacted conditions which can permit evaluation of the role of soil structure on the shape of the compression curve and relationship between suction and yield stress.

BACKGROUND

Stresses in Unsaturated Soil

The effective stress principle is used to apply solid mechanics principles to porous media like soils. Terzaghi (1923) defined the effective stress to be a single value of stress that govern the elastic volume change, shear strength, and stiffness in soil as follows:

$$\sigma' = \sigma - u_w \tag{1}$$

where σ' is the effective stress, σ is the total stress, and u_w is the pore water pressure. Bishop (1959) extended the effective stress to unsaturated soil as follows:

$$\sigma' = (\sigma - u_a) + \chi(u_a - u_w) \tag{2}$$

where u_a is the pore air pressure, $\psi = (u_a - u_w)$ is the matric suction, $(\sigma - u_a)$ is the net stress, χ is the effective stress parameter. Bishop (1959) proposed that the parameter χ to be the degree of saturation, however, Coleman (1962) stated that the effective stress parameter is related to the soil structure and does not have a direct correlation with the degree of saturation. Khalili & Zargarbashi (2010) found from the results of multi-stage triaxial tests that the relationship between the effective stress parameter and degree of saturation may not be unique due to hydraulic hysteresis. Liu et al. (2020) used discrete element modeling to calculate the effective stress parameter using the average contact stress and found that it matches the degree of saturation very well, in contrast to the conclusion from Coleman (1962). Bolzon & Schrefler (1995) improved

Bishop's (1959) definition by proposing that χ is the effective saturation, which Lu et al. (2010) found permits integration of the soil-water retention curve (SWRC) into the effective stress definition. For example, the effective saturation can be represented using the van Genuchten (1980) SWRC model:

$$S_e = \frac{S - S_r}{1 - S_r} = \left[\frac{1}{1 + (\alpha_{vG}\psi)^{N_{vG}}}\right]^{\frac{1}{1-N_{vG}}} \quad (3)$$

where S_e is the degree of saturation, S_r is the residual degree of saturation, and α_{vG} and N_{vG} are parameters of the van Genuchten (1980) SWRC model. Lu et al. (2010) also noted that Equation (2) can be written in the following form:

$$\sigma' = (\sigma - u_a) + \sigma_s \quad (4)$$

where σ_s is defined as the suction stress. The suction stress can be calculated as the product of the measured suction and effective saturation during an experiment, or may be predicted by integrating the SWRC from Equation (3) into Equation (2).

Volume Change of Unsaturated Soils

Most early studies on the compression response of unsaturated soils focused on the collapse response of compacted soils (Jennings & Knight 1957; Jennings & Burland 1962; Matyas & Radhakrishna 1968; Dudley 1970; Houston et al. 2001) and involved the use of double oedometer tests where one compacted specimen was soaked then loaded to high stresses and another was loaded to high stresses and soaked. These studies raised concerns about the applicability of the effective stress principle to unsaturated soils because a volumetric contraction (collapse) was observed in the loaded then soaked specimen during wetting, corresponding to a reduction in effective stress. Accordingly, constitutive models like the Barcelona Basic Model (BBM) of Alonso et al. (1990) and Wheeler and Sivakumar (1995) were developed to consider the effects of suction and net stress on volume change independently. A key part of the model was a yield curve in the net stress and suction space, referred to as the loading-collapse (LC) curve, with a shape developed based on data for compacted soils that was linked to the slope of the compression curve after yielding. Khalili et al. (2004) rebutted the concerns about using the effective stress principle to capture the compression response of unsaturated soils and noted that a 1:1 relationship between effective stress and volume change is only required for elastic conditions, and that appropriate elasto-plastic frameworks can consider the collapse upon wetting phenomena in effective stress terms. Khalili et al. (2004) noted that suction has independent effects on the effective stress in Equation (2) and on the yield stress in the LC curve, and that soils who have a greater increase in yield stress with suction than the rate of increase in effective stress with suction can be considered collapsible. Recent constitutive models for unsaturated soils have used the effective stress principle (e.g., Wheeler et al. 2003) and several models for the LC curve have been proposed in terms of effective stress (e.g., Wheeler et al. 2003; Salager et al. 2008; Tourchi and Hamidi 2015). While the overconsolidation ratio (OCR) is often used in constitutive modeling of saturated soils, the dual effects of suction on the effective stress and yield stress imply that it is difficult to use this parameter in the interpretation of data. Nonetheless, Wu et al. (2019) found that the shear strength of unsaturated sedimented soils depends on the OCR prior to desaturation.

Although soil structure may have a significant impact the compression response of unsaturated soils, most constitutive models for unsaturated soils are generally formulated around and calibrated using the experimental data from compacted soils (Alonso et al. 1990; Wheeler & Sivakumar 1995; Cui et al. 1995; Bolzon et al. 1996; Gallipoli et al. 2003; Zhou et al. 2012a, 2012b). Sheng et al. (2008) modified the BBM to include the yield stress effect for soils that are consolidated from a slurry state and for soils that are compacted at a suction above the saturation suction. The modified model showed that the yield stress of soils that are initially compacted will have higher yield stress with increasing suction than soils consolidated from a slurry. McCartney & Behbehani (2021) collected and analyzed compression curves from 25 studies in the literature for compacted and sedimented unsaturated soils to understand the impacts of suction on the suction stress at yielding, the apparent yield stress, and slope of the vertical compression line. In general, both sedimented and compacted soils showed an increase in yield stress with suction, and that suction generally had a greater impact on the yield stress than on the suction stress, but it was not possible to compare the role of soil preparation techniques on these variables for a single soil. McCartney & Behbehani (2021) noted that it was important to measure the degree of saturation during compression to interpret the compression curves in terms of effective stress.

Mun and McCartney (2017) proposed a general hypothetical representative of the drained hydro-mechanical compression response of compacted soils to high stresses, which was adapted in Figure 1 for the case of soils sedimented from a slurry, unloaded, desaturated to different suction, then loaded to high stresses. The hypothetical compression curves in Figure 1(a) start in a saturated slurry condition that undergoes self-weight consolidation following a nonlinear path that eventually stabilizes and follows the log-linear virgin compression line (VCL). After loading to a state that is clearly on the VCL, the specimens are unloaded to provide an initial point of comparison with the compression response of compacted soils. The suction is then applied which will lead to a decrease in the degree of saturation and an increase in effective stress as shown in the hypothetical curves in Figure 1(b). Each applied suction will thus lead to a different starting point on the recompression curve. While a saturated specimen is expected to yield at the same stress from which the soil had been unloaded, the unsaturated specimens are expected to have a yield stress that depends on the suction and the soil structure induced by sedimentation. During drained compression, the degree of saturation will typically increase as the volume of voids decreases, although some water outflow and reduction in the volume of water may also occur for soils with higher initial degrees of saturation making it important to track outflow. Soils with lower initial degrees of saturation typically do not experience outflow of water and can be assumed to have constant water content. Greater increases in degree of saturation are expected after yielding (Wheeler et al. 2003). After yielding, the compression curves for unsaturated soils are expected to converge with the compression curve for saturated soils at mean stresses greater than 10 MPa (Mun and McCartney 2017). However, the review of compression response of unsaturated soils reported by McCartney and Behbehani (2021) indicates that the compression curves are highly nonlinear and depending on the maximum stress applied the curves may show a diverging trend (e.g., Maatouk et al. 1995) or a parallel trend (e.g., Sharma 1998; Rampino et al. 1999).

EXPERIMENTAL INVESTIGATION

Material and Specimen Preparation

The silt investigated in this study was collected from the Bonny dam on the Colorado–Kansas border. Although several previous studies have investigated the volume change response of compacted Bonny silt specimens having different compaction conditions, initial degrees of saturation, and temperatures (Khosravi & McCartney 2011: Vega et al. 2012; Alsherif & McCartney 2015; Khosravi et al. 2016; Coccia & McCartney 2016), the compression response of unsaturated Bonny silt specimens consolidated from a slurry has not yet been investigated. Bonny silt is classified as ML (inorganic low plasticity silt) according to the Unified Soil Classification System (USCS, ASTM D2487), and relevant index properties of Bonny silt are given in Table 1. The silt has a relatively low air entry suction of less than 10 kPa and does not reach residual saturation until approximately 1000 kPa, making it well suited for the suction range of the axis translation technique.

Experiment Setup

To accommodate both large-strain consolidation and desaturation of soils using the axis translation technique, a new oedometer was developed for use in a triaxial pressure cell, as shown in Figure 2(a). The base platen of the triaxial cell was adapted to accommodate a central high-air entry porous disc for use in the axis translation technique, and a concentric outer coarse porous stone that permits larger water flow rates anticipated during consolidation from a slurry. The air entry suction of the high air entry ceramic disc has a capacity of 300 kPa, which was deemed to be a sufficiently high capacity to characterize the funicular regime of the SWRC. The outer diameter of the 35 mm-tall base platen has two “O”-ring grooves which provide a seal with a slip-fit specimen tube having a height of 175 mm, an inner diameter of 70 mm, and a wall thickness of 15 mm as shown in Figure 2(b). The base platen and specimen tube were fabricated from anodized aluminum. The wall thickness of the specimen tube was selected to have sufficient rigidity to minimize radial strains induced by application of high axial stresses up to 11 MPa to the soil specimen. A coarse porous stone having a thickness of 17 mm is to use provide drainage from the top of the specimen, and a slip fit top platen made from anodized aluminum is used to distribute the force from the piston of the triaxial cell. The slip fit of the top platen is designed to prevent tilting during large strain consolidation while still allowing drainage of water or air from the top of the specimen. A linearly variable differential transformer (LVDT) is connected to the top of the specimen tube within the pressure cell, with the core resting on the top platen. Axial stresses are applied to the soil specimen using a 44.5 kN load frame in displacement control mode as shown in Figure 2(c), and an S-type load cell is used to record the force applied to the piston of the triaxial cell. The triaxial cell pressure, which is also the air pressure in the axis translation technique when desaturating the soil specimen, is applied using a pressure panel. A flow pump is used to control the water pressure at the base of the soil specimen. During compression under saturated conditions, the flow pump is connected to the coarse porous stone in the bottom platen, while during desaturation, the flow pump is connected to the high air entry porous stone. The flow pump has pressure and volume control capabilities, has a volumetric capacity of 75 ml, a maximum flowrate of 25 ml/min, and can apply pressures between -100 to 2070 kPa. The flow pump incorporates a pressure sensor that can be used for maintaining constant pressures with the pump via a feedback loop. A pore pressure transducer (PPT) is attached to the coarse porous stone to record the pressure at the base of the specimen during consolidation and desaturation. During desaturation, the measurements from this PPT do not provide a meaningful quantification of the pore air or water pressures, but as will be shown in the results section was useful in detecting the point of air entry into the soil. Pictures of the setup within the triaxial cell are shown in Figure 3.

Experimental Procedures

The soil specimens were prepared by initially drying them at 100°C for 24 hours, cooling to room temperature, and crushing any agglomerates with a mortar and pestle so that it passes a 2 mm sieve opening. Then the dry soil was mixed with tap water to reach a water content of two times the liquid limit. The slurry was poured into the specimen tube and covered to prevent any water loss and then left to homogenize and consolidate under its self-weight for 48 hours. The slurry specimens initially had heights between 37.5 and 40.0 mm high, and 70 mm diameter wide. The initial gravimetric water contents of the slurries ranged from 49 to 51%. After self-weight consolidation, the soil was sufficiently stiff to support the weight of the coarse porous stone and the top platen. At this stage, the cell was assembled and filled with water just below the top of the specimen tube so that the LVDT would remain dry. A constant initial backpressure of 172.4 kPa was applied to the air in the upper portion of the cell using the pressure control panel and to the specimen base using the flow pump. In the initial stage of the test, the cell/air pressure is conveyed to the water on top of the soil layer. The backpressure was applied to ensure that any air dissolved in the water remained dissolved after passing out of the specimen during desaturation using the axis translation technique.

All sedimented soil specimens were initially loaded in saturated conditions to 420 kPa at a constant displacement rate of 1.8 mm/day (axial strain rates of 4.5 to 4.8 %/day) then unloaded to zero applied axial stress. The hydro-mechanical behavior of unsaturated soils is related to the strain rate at which the experiment is conducted, as the compression curve is defined as the relationship between void ratio and effective stress at hydraulic equilibrium after any excess pore water pressures due to mechanical loading have dissipated. Many experiments were conducted to understand the loading rate influence on unsaturated soil specimens. For example, the strain rate can affect the yield stress value and the compression behavior of the specimen (Qin et al. 2015), and at high suction levels, the loading rate will change the soil stiffness (Rojas & Mancuso 2009). Wu et al. (2020) showed that increasing the strain rate will lead to decrease the degree of saturation and the volumetric strain of the unsaturated specimen at the critical state. The displacement rate during loading of 1.8 mm/day was found to be sufficient to minimize the build-up of pore water pressure during both consolidation of the slurry and later compression of the unsaturated soil as measured by the PPT in the coarse porous stone. Unloading was performed at half the rate during compression following recommendations in ASTM D4186/D4186M. The typical frame movement during this initial loading and unloading process is shown in the schematic time series Figure 4(a). Suctions values ranging from 0 to 270 kPa were the applied to the specimen and time was permitted for desaturation. The time required for reaching equilibrium of water outflow from the base required different times, which is why Figure 4 is shown without a time scale for ease of comparisons between controlled variables in the different tests. To apply the suction values, the water pressure at the base of the specimen (applied through the high air entry ceramic) was maintained at 172.4 kPa and the air pressure was elevated to different values as shown in Figure 4(b). This led to the application of different suction values as shown in Figure 4(c). After reaching equilibrium of water outflow during desaturation under the different suction values, the specimens were reloaded to a vertical effective stress of approximately 11 MPa at a rate of 1.8 mm/day then unloaded to finish the test. The maximum load was selected to encompass the range of the stresses encountered in near-surface geotechnical engineering applications of approximately 10 MPa.

RESULTS

The actual time series from the desaturation phase in the tests on specimens with different suction magnitudes is shown in Figure 5. During consolidation of the soil from a slurry, the specimen is double drained, so water can flow freely upward through the top coarse porous stone and downward through the outer coarse porous stone as the pump maintains a constant pressure. The outflow volume from the base can be tracked from the pump position. The flow pump maximum speed was set to be 0.1 ml/min, which was sufficiently fast to maintain a constant pressure of 172.4 kPa during outflow but slow enough to avoid overshooting. As mentioned, the water that is drained through the top stone is stored above the soil layer in the specimen tube. After application of the difference in air and water pressures shown in Figure 4(b), a gradient is induced across the saturated specimen, and the water above the specimen starts to flow downward through the specimen and out of the high air entry ceramic disc to the flow pump. As all the applied suctions are greater than the air entry suction, air will eventually enter the soil and the water outflow will gradually decrease until reaching equilibrium. Time series of water outflow and calculated degree of saturation in the different tests are shown in Figure 5(a), which indicates that equilibrium is typically reached after 60 hours. As the specimens are all initially saturated and overconsolidated, the specimens were relatively stiff. The changes in height during application of the greatest suction was less than 2×10^{-7}m. Accordingly, the volume of voids had a negligible change so the volume of water flowing out of the specimen and the degree of saturation were observed to follow similar but inverted trends in Figure 5(a). The pump pressure, controlled via the port connected to the high air entry ceramic during desaturation, is shown together with the degree of saturation in Figure 5(b), which indicates that the pump pressure is generally constant but that greater fluctuations with a maximum amplitude of ±15 kPa occur when large amounts of water outflow is occurring during the early stage of desaturation. An interesting observation was made from the PPT attached to the coarse porous stone during the desaturation phase shown together with the degree of saturation in Figure 5(c). This sensor is not measuring the air or water pressure, but a value between the two applied values. A temporary drop in pressure was observed to coincide with the point of air entry. During desaturation, the pump (water) and cell (air) pressures are maintained constant, and any water outflow is permitted to drain to the flow pump due to the lower water pressure. The water outflow and the volume of voids were used to track the degree of saturation during compression, as will be shown later. The PPT attached to the coarse porous stone indicated that the pressure remained steady during compression, indicating that the rate of compression was slow enough to maintain drained conditions. The tests on the specimens at suctions of 0 (saturated) 20 kPa were performed first before the testing procedures were refined, and unfortunately were stopped before reaching 11 MPa without recording of the during unloading. At the end of the tests, the final dimensions of the specimen and the gravimetric water content were measured.

The compression curves for the sedimented Bonny silt specimens are shown in Figure 6(a) in terms of effective stress calculated using the sum of the applied net stress and the product of the applied suction and measured degree of saturation. Because the test was performed over a wide range of stresses and void ratios, the portions of the compression curves during initial consolidation of the slurry up to 420 kPa are shown in Figure 6(b) while the portion during suction application and subsequent loading to approximately 11 MPa is shown in Figure 6(c). All the compression curves are shown in terms of the change in void ratio with respect to the initial slurry void ratio as due to slight differences in the initial void ratios of the slurries and specimen dimensions. The initial compression curves in Figure 6(b) have different slopes at very low stresses due to the fragile condition of the slurry and because the loads were close to the lower limit of the load cell. However, at around 300 kPa, the compression curves converge and follow a similar path. The compression index is approximately 0.24 for the saturated soil which is similar to oedometer tests on saturated Bonny silt specimens compacted dry of optimum (Alsherif & McCartney 2015). During the transient desaturation stage shown in Figure 6(c), the effective stress will initially equal to the applied suction as the degree of saturation is initially 1 and the axial load is zero. However, the effective stress will reduce over time as water flows out of the soil and the degree of saturation reaches equilibrium, as shown in Figure 6(c). Consistent with observations from compacted soils, the recompression curves in Figure 6(c) indicate that the applied suction does lead to an increase in yield stress for sedimented soils, with the yield stress defined using the approach of Casagrande (1946). An interesting observation is that in the range of axial stresses applied, the slopes of the VCLs for unsaturated specimens were either parallel to that of the saturated soil specimen or slightly diverged. This was consistent with the compression curves for compacted Bonny silt specimens tested by Coccia & McCartney (2016) and Khosravi et al. (2018). This observation is not consistent with the hypothetical compression curves in Figure 1(a) but could be attributed to the nonlinearity of the compression curves and the fact that larger axial stresses may be necessary to reach pressurized saturation and air expulsion. The water outflow during the reloading of the specimens with different suction values is shown in Figure 6(d). Specimens with higher suction values have lower amounts of water outflow mainly as there is less water in the soil and water is held at the particle contacts. The suction stress calculated as the product of the degree of saturation and suction is shown in Figure 6(e) as a function of total vertical stress. This figure shows that the initial suction stress increases with applied suction, and that the rate of change in suction stress with net stress depends on the initial suction of the soil due to the trends in water outflow observed in Figure 6(d).

The hydro-mechanical behavior of the unsaturated soil specimens during the compression stage is shown in Figure 7. A plot of the applied matric suction versus the change in void ratio is shown in Figure 7(a), for the portion of the compression curve focused on unsaturated conditions shown in Figure 6(c). As the suction was constant during compression, the relationships between the change in void ratio and suction are vertical lines. Smaller changes in void ratio occur during compression to 11 MPa for increasing suction, which can be attributed to the shallower slopes of the VCL for unsaturated specimens at high stresses observed in Figure 6(c). A maximum change in void ratio of 1.217 was observed for the saturated specimen while a minimum change in void ratio of 1.003 was observed for the specimen with a suction of 270 kPa. The degree of saturation versus the change in void ratio during the desaturation and recompression stages is shown in Figure 7(b). As noted, there was not a significant change in void ratio during desaturation, but recompression led to an increase in the degree of saturation. In the tests on specimens at 20 and 40 kPa, the specimens reached saturation (S=1) during recompression, while in the other tests, an increase was observed but saturation was not reached. The curves in Figure 7(c) show the transient loops of degree of saturation versus the effective stress. The curves are initially inclined downward during the transient desaturation process shown in Figure 6(b), after which the degree of saturation increases nonlinearly while the vertical effective stress increases. A major increase in degree of saturation does not occur until reaching yielding, as noted in Figure 1(b). During unloading, the degree of saturation rebounded slightly in the tests on the specimens with high suction values, forming a loop. The changes in degree of saturation with effective stress follow generally parallel slopes prior to yielding, then the specimens with initially higher suction values show a more rapid increase in degree of saturation during compression.

ANALYSIS

The equilibrium values of suction and degree of saturation prior to recompression in each of the specimens permits definition of points on the SWRC for sedimented Bonny silt, as shown in Figure 8(a) along with the best-fit van Genuchten (1980) SWRC from Equation (3) obtained using fitting parameters of $\alpha_{vG} = 0.025\ \text{kPa}^{-1}$ and $N_{vG} = 1.64$. A comparison of the best fit SWRC for the sedimented Bonny silt is compared with two SWRCs reported in the literature for compacted Bonny silt in Figure 8(b). The sedimented specimen had an air entry suction of approximately 10 kPa, which is greater than that of the compacted specimens, which were approximately 1 to 2 kPa. The high air entry suction for the sedimented specimen could be related to a dispersed structure associated with initial compression of the slurry to 420 kPa. An interesting observation is that the fitting parameter N_{vG} for the sedimented Bonny silt was similar to those defined by Alsherif & McCartney (2016) and Başer et al. (2018) for compacted Bonny silt. The parameter N_{vG} is related to the pore size distribution of the soil, indicating that the sedimented and compacted Bonny silt specimens may have different soil structures but similar pore size distributions.

A relationship between the yield stress and the degree of saturation at yielding for the sedimented Bonny silt is shown in Figure 9(a), along with similar relationships for compacted

Bonny silt from the literature. The dry unit weight for the sedimented specimen attained after compression to 420 kPa is 16.1 kN/m^3, which is greater than the dry unit weights of 14.22 and 14.05 kN/m^3 reported by Coccia and McCartney (2016) and Khosravi et al. (2018) for compaction at a gravimetric water content of 14%. Although this compaction gravimetric water content corresponds to the optimum water content for the standard Proctor compaction curve as noted in Table 1, the lower dry unit weights investigated in these studies indicates that this gravimetric water content likely corresponds to dry of optimum conditions for this effort. The yield stresses for the sedimented specimens are consistent greater than those of the compacted specimens, potentially due to the higher initial dry unit weight associated with sedimentation. Additionally, both Coccia and McCartney (2016) and Khosravi et al. (2018) measured the compression curves in isotropic stress states, which may lead to a softer response than in oedometric conditions. The yield stresses of the sedimented and compacted Bonny silt specimens are shown as a function of matric suction on a 1:1 scale in Figure 9(b). Although Uchaipichat and Khalili (2009) noted that the yield stress should not increase from the value at saturation until reaching the air entry suction, this feature was not well observed in the data because the air entry suction of the soil was below the lowest value of suction applied. As the yield-stress vs. suction relationships were approximately linear over the range of suctions applied, and because the air entry suction is relatively small compared to range of applied suctions, the linear LC curve of Tourchi & Hamidi (2015) model was fitted to the data. Their LC curve is given as follows:

$$\sigma'_y(\psi) = \sigma'_y(\psi_0) + \varpi\psi \tag{5}$$

where $\sigma'_y(\psi)$ is the effective yield stress at any suction, $\sigma'_y(\psi_0)$ is the yield stress at zero suction (saturation), and ϖ is a fitting parameter representing the slope of the LC curve. Although there is some scatter in the data, the slopes of the LC curves for the compacted and sedimented Bonny silt specimens were similar with a value of $\varpi = 1.7$. This observation may be related to the similar N_{vG} parameters for the compacted and sedimented silt specimens reflecting similar pore size distributions despite the different soil structures associated with the preparation technique.

As Khalili et al. (2004) noted that unsaturated soils can be categorized based on whether suction has a greater effect on the yield stress or the effective stress, the suction stress at the point of yielding (defined as the product of the measured degree of saturation and applied matric suction) is shown in Figure 10. Similar curves for the compacted Bonny silt specimens are also shown in this figure, which indicate a clear overlap with the curve for sedimented Bonny silt specimens. The results in this figure indicate that the suction has a much greater effect on the yield stress than the suction stress (and thus the effective stress) for both the compacted and sedimented Bonny silt specimens. This indicates that the sedimented and compacted Bonny silt specimens would both be collapsible.

The compression indices for the specimens with different constant matric suction values are shown in Figure 11 for the compacted and sedimented Bonny silt specimens. As noted in the evaluation of the compression curves in Figure 6(c), a decreasing trend in the compression indices is noted with increasing suction, indicating that the compression curves are diverging, and not converging as shown in the hypothetical compression curves in Figure 1(a). This is likely because the stress range applied in this study is not sufficient to lead to the transition to pressurized saturation. The compression indices for the sedimented soils were greater than those for the compacted soils, indicating that they will be stiffer with less changes in volume for the same changes in stress. Although there is a large difference in the slopes of the curves of the sedimented specimens with suctions greater than 40 kPa and the ones at 0 and 20 kPa, the trend in compression index with suction in the higher suction range is similar to that observed in the studies on the compacted Bonny silt specimens. This further adds to the possibility that the sedimented and compacted Bonny silt specimens have similar pore size distributions despite the differences in preparation technique.

CONCLUSIONS

A comparison between the compression curves of sedimented and compacted Bonny silt in terms of effective stress provided new insights into the impacts of specimen preparation on the yielding response of unsaturated soils. An increase in apparent yield stress with suction was observed for both the saturated and unsaturated soils. After yielding, the compression curves for specimens with higher suctions diverged without tending toward pressurized saturation in the applied axial stress range of 11 MPa. Sedimented soils were found to have greater yield stresses in both saturated and unsaturated conditions when compared with soils compacted dry of optimum, which may have occurred due to the greater initial dry unit weight of the sedimented soils. However, a similar increase in yield stress with suction was observed for both the sedimented and compacted soils. Sedimented soils also experienced smaller changes in volume with applied stress and higher air entry suction value than compacted soils, possibly due to a denser, dispersed soil structure. However, similar pore size parameters in the SWRC, similar slopes of the yield stress versus suction relationship, and similar changes in the compression index with suction indicate that the compacted and sedimented soils may have similar pore size distributions. Suction was found to have a greater impact on yield stress than suction stress for both sedimented and compacted soils, indicating that they are both susceptible to collapse upon wetting.

ACKNOWLEDGMENTS

The first author would like to acknowledge the doctoral scholarship and support provided by Kuwait University.

DATA AVAILABILITY STATEMENT

All data, models, and code generated or used during the study appear in the submitted article.

REFERENCES

Ahmed, S., Lovell Jr, C. W., & Diamond, S. (1974). "Pore sizes and strength of compacted clay." Journal of the Geotechnical Engineering Division, 100(4), 407-425.

Al-Mukhtar, M., Alcover, J.-F., & Berbaya, F. (1999). "Oedometric and water-retention behavior of highly compacted unsaturated smectites." Canadian Geotechnical Journal, 36(11), 675–684.

Alonso, E.E., Gens, A., & Josa, A. (1990). "A constitutive model for partially saturated soils." Géotechnique, 40(3), 405-430.

Alsherif N.A., & McCartney, J.S. (2016) "Yielding of silt at high temperature and suction magnitudes." Geotechnical and Geological Engineering, 34(2), 501-514.

Başer, T., Dong, Y., Moradi, A. M., Lu, N., Smits, K., Ge, S. & McCartney, J.S. (2018). "Role of nonequilibrium water vapor diffusion in thermal energy storage systems in the vadose zone." Journal of Geotechnical and Geoenvironmental Engineering, 144(7), 04018038.

Bishop, A.W. (1959). "The principle of effective stress." Teknisk ukeblad, 39, 859-863.

Bolzon, G., & Schrefler, B.A. (1995). "State surfaces of partially saturated soils: an effective pressure approach." Applied Mechanics Reviews, 48(10), 643-649.

Bolzon, G., Schrefler, B. A., & Zienkiewicz, O. C. (1996). "Elastoplastic soil constitutive laws generalized to partially saturated states." Géotechnique, 46(2), 279-289.

Casagrande, A. (1936). "The determination of the preconsolidation load and its practical significance." Proc., 1st Int. Conf. on Soil Mech. and Found. Eng., Vol. 3, Balkema, Rotterdam, The Netherlands, 60–64.

Coccia, C.J.R. & McCartney, J.S. (2016). "Thermal volume change of poorly draining soils I: Critical assessment of volume change mechanisms." Computers and Geotechnics, 80(12), 26-40.

Coleman, J.D. (1962). "Stress strain relations for partly saturated soil." Correspondence to Geotechnique, 12(4), 348-350.

Cui, Y. J., Delage, P., & Sultan, N. (1995). "An elasto-plastic model for compacted soils." In Proc. of the 1st International Conference on Unsaturated Soils, Vol. 2, 703-709. Balkema, Rotterdam.

Cuisinier, O., & Masrouri, F. (2005). "Hydromechanical behaviour of a compacted swelling soil over a wide suction range." Engineering Geology, 81(3), 204-212.

Cunningham, M. R., Ridley, A. M., Dineen, K., & Burland, J. B. (2003). "The mechanical behaviour of a reconstituted unsaturated silty clay." Géotechnique, 53(2), 183-194.

Delage, P., Audiguier, M., Cui, Y. J., & Howat, M. D. (1996). "Microstructure of a compacted silt." Canadian Geotechnical Journal, 33(1), 150-158.

Dudley, J.H. (1970). "Review of collapsing soils." Journal of Soil Mechanics and Foundation Engineering, ASCE(SM3), 925-947.

Fleureau, J.M., Kheirbek-Saoud, S., Soemitro, R., & Taibi, S. (1993). "Behaviour of clayey soils on drying-wetting paths." Canadian Geotechnical Journal, 30(4), 287–296.

Gallipoli, D., Gens, A., Sharma, R., & Vaunat, J. (2003). "An elasto-plastic model for unsaturated soil incorporating the effects of suction and degree of saturation on mechanical behaviour." Géotechnique, 53(1), 123-135.

Gao, Y., Sun, D.A., & Zhou, A. (2016). "Hydromechanical behaviour of unsaturated soil with different specimen preparations." Canadian Geotechnical Journal, 53(6), 909-917.

Geiser, F., Laloui, L., & Vulliet L. (2006). "Elasto-plasticity of unsaturated soils: laboratory test results on a remoulded silt." Soils and Foundations, 46(5), 545-556.

Houston, S.L., Houston, W.N., Zapata, C.E., & Lawrence, C. (2001). Geotechnical engineering practice for collapsible soils. In: Toll, D.G. (eds) Unsaturated Soil Concepts and Their Application in Geotechnical Practice. Springer, Dordrecht. 333-355.

Jennings, J.E.B., & Burland, J.B. (1962). "Limitations to the use of effective stresses in partly saturated soils." Géotechnique, 12(2), 125-144.

Jennings, J.E.B., & Knight, K. (1957). "The additional settlement of foundations due to a collapse of structure of sandy subsoils on wetting." Proc. 4^{th} Int. Conf. Soil Mech., Vol. 1, 316-319. Butterworths, London.

Jotisankasa, A., Ridley, A., & Coop, A. (2007). "Collapse behavior of a compacted silty clay in the suction-monitored oedometer apparatus." Journal of Geotechnical and Geoenvironmental Engineering, 133(7), 867-877.

Khosravi, A., Sajjad, S., Dadashi, A., & McCartney, J.S. (2016). "Evaluation of the impact of drainage-induced hardening on the small strain shear modulus of unsaturated soils." International Journal of Geomechanics, 16(6), D4016007.

Khalili, N., Geiser, F., & Blight, G.E. (2004). "Effective stress in unsaturated soils, a review with new evidence." International Journal of Geomechanics, 4(2), 115-126.

Khalili, N. & Zargarbashi, S. (2010). "Influence of hydraulic hysteresis on effective stress in unsaturated soils." Géotechnique, 60(9), 729–734.

Khosravi, A., Rahimi, M., Gheibi, A., & Shahrabi, M.M. (2018). "Impact of plastic compression on the small strain shear modulus of unsaturated silts." International Journal of Geomechanics, 18(2), 04017138.

Liu, X., Zhou, A., Shen, S.L., Li, J. & Sheng, D. (2020). “A micro-mechanical model for unsaturated soils based on DEM”. Computer Methods in Applied Mechanics and Engineering, 368, p.113183.

Lloret, A., Villar, M.V., Sanchez, M., Gens, A., Pintado, X., & Alonso, E.E. (2003). “Mechanical behaviour of heavily compacted bentonite under high suction changes.” Géotechnique, 53(1), 27-40.

Lu, N., Godt, J., & Wu, D. (2010). “A closed-form equation for effective stress in unsaturated soil.” Water Resources Research, 46(5), 1–14.

Maâtouk, A., Leroueil, S., & La Rochelle, P. (1995). “Yielding and critical state of collapsible unsaturated silty soil.” Géotechnique, 45(3), 465–477.

Matyas, E.L., & Radhakrishna, H.S. (1968). “Volume change characteristics of partially saturated soils.” Géotechnique, 18(4), 432–448.

McCartney, J.S., & Behbehani, F. (2021). “Hydromechanical behavior of unsaturated soils: Interpretation of compression curves in terms of effective stress.” Soils and Rocks, 44(3), e2021065721

Mitchell, J.K., Hooper, D.R., & Campanella, R.G. (1965). “Permeability of compacted clay.” ASCE Journal of the Soil Mechanics and Foundations Division (JSMFD), 91(SM4), 41-65.

Mun, W. & McCartney, J.S. (2017). “Constitutive model for the drained compression of unsaturated clay to high stresses.” Journal of Geotechnical and Geoenvironmental Engineering, 143(6), 04017014.

Qin, P.J., Ye, W.M., Chen Y.G., Chen B., & Cui, Y.J. (2015). “Influence of strain-rate on hydromechanical behavior of highly compacted GMZ01 bentonite”. Eng Geol 195:85–92

Rampino, C., Mancuso, C., & Vinale, F. (1999). "Laboratory testing on an unsaturated soil: equipment, procedures, and first experimental results." Canadian Geotechnical Journal, 36(8), 1–12.

Rojas, J.C., & Mancuso, C. (2009). "Effect of loading rate on the behaviour of unsaturated soils". In: Hamza H (ed) Proceedings of the 17th international conference on soil mechanics and geotechnical engineering. IOS Press, Amsterdam, pp 761–764

Salager, S., François, B., El Youssoufi, M.S., Laloui, L. & Saix, C. (2008). "Experimental investigations of temperature and suction effects on compressibility and pre-consolidation pressure of a sandy silt." Soils and Foundations, 48(4), 453-466.

Sharma, R. (1998). Mechanical Behaviour of Unsaturated Highly Expansive Soil, PhD Thesis, University of Oxford, UK.

Sheng, D., Fredlund, D. G., & Gens, A. (2008). "A new modelling approach for unsaturated soils using independent stress variables." Canadian Geotechnical Journal, 45(4), 511-534.

Shanina, M. & McCartney, J.S. (2017). "Influence of anisotropic stress states on the thermal volume change of unsaturated silt." Soils and Foundations, 57(2), 252-266.

Tarantino, A., & De Col, E. (2008). "Compaction behaviour of clay." Géotechnique, 58(3), 199-213.

Tarantino, A. (2010). "Unsaturated soils: compacted versus reconstituted states." In 5th International Conference on Unsaturated Soil. pp. 113-136. Balkema, Rotterdam.

Thu, T. M., Rahardjo, H., & Leong, E. C. (2007). "Critical state behavior of a compacted silt specimen." Soils and Foundations, 47(4), 749-755.

Tourchi, S., & Hamidi, A. (2015). “Thermo-mechanical constitutive modeling of unsaturated clays based on the critical state concepts.” Journal of Rock Mechanics and Geotechnical Engineering, 7(2), 193-198.

Terzaghi, K. (1923). “Discussion of lateral earth pressure: the accurate experimental determination of the lateral earth pressure, together with a resume of previous experiments.” Transactions of the American Society of Civil Engineers, 86, 1525-1543.

Uchaipichat, A. & Khalili, N. (2009). “Experimental investigation of thermo-hydro-mechanical behaviour of an unsaturated silt.” Géotechnique, 59(4), 339-353.

van Genuchten, M.T. (1980). “A closed form equation for predicting the hydraulic conductivity of unsaturated soils.” Soil Science Society of America Journal, 44(5), 892-898.

Wheeler, S.J. & Sivakumar, V. (1995). “An elasto-plastic critical state framework for unsaturated soils.” Géotechnique, 45(1), 35-53.

Wheeler, S.J., Sharma, R.J. & Buisson, M.S.R. (2003). “Coupling of hydraulic hysteresis and stress-strain behaviour in unsaturated soils.” Géotechnique, 53(1), 41-54.

Wu, S. Zhou, A., Li, J., Kodikara, J., and Cheng. W.-C. (2019). “Hydromechanical behaviour of overconsolidated unsaturated soil in undrained conditions.” Canadian Geotechnical Journal. 56(11), 1609-1621.

Wu, S., Zhou, A., Shen, S.L. & Kodikara, J. (2020). “Influence of different strain rates on hydro-mechanical behaviour of reconstituted unsaturated soil”. Acta Geotechnica, 15(12), 3415-3431.

Zhou, A.-N., Sheng, D., Sloan, S.W., & Gens, A. (2012a). “Interpretation of unsaturated soil behaviour in the stress – saturation space, I: Volume change and water retention behavior.” Computers and Geotechnics, 43, 178-187.

Zhou, A-N., Sheng, D., Sloan, S.W., & Gens, A. (2012b). "Interpretation of unsaturated soil behaviour in the stress – saturation space, II: Constitutive relationships and validations." Computers and Geotechnics, 43, 111-123.

TABLE 1: Geotechnical properties of Bonny silt.

Parameter	Value
D_{10}	<0.0013 mm
D_{30}	0.022 mm
D_{50}	0.039 mm
% Passing No. 200 sieve	83.9
% Clay size	14
% Silt size	69.9
% Sand size	16.1
Liquid limit, LL	25
Plastic limit, PL	21
Plasticity index, PI	4
Maximum dry unit weight* (γ_{dry})	16.3 kN/m^3
Optimum water content* (w_{opt})	14%

*Defined according to the standard Proctor compaction effort

FIG. 1: Hypothetical hydro-mechanical behavior of unsaturated soils during drained compression with constant suction: (a) Compression curves in terms of effective stress of unsaturated soils during drained compression with constant suction; (b) Increases in degree of saturation during drained compression.

FIG. 2: Experimental setup for the custom oedometer for unsaturated soils within a pressure cell: (a) Schematic of the oedometer in the triaxial cell; (b) Detailed schematic of oedometer body; (c) Schematic showing connections from the triaxial cell to the pressure panel and flow pump.

FIG. 3: Pictures of the custom oedometer for unsaturated soils within a pressure cell setup: (a) Picture of the assembled setup; (b) Picture of the oedometer setup; (c) Picture showing the hydraulic connections from the cell to the pressure panel and flow pump.

FIG. 4: Schematic time series for variables controlled in tests on specimens with different suctions: (a) Load frame movement; (b) Pore water and pore air pressures; (c) Applied suction.

FIG. 5: Time series during desaturation for the tests with different suctions: (a) Changes in the volume of water outflow and degree of saturation; (b) Pore water pressure and degree of saturation results; (c) Fluid pressure at the base and degree of saturation.

FIG. 6: Compression curves for sedimented Bonny silt specimens; (a) Full compression curves; (b) Initial portions during slurry consolidation (all specimens are fully saturated); (c) Portions during and after desaturation showing transient suction application effects and yield stresses; (d) Water outflow during compression of unsaturated specimens; (e) Suction stress during compression of unsaturated specimens.

FIG. 7: Hydro-mechanical behavior of sedimented Bonny silt during compression at different matric suction values: (a) Changes in void ratio with matric suction; (b) Changes in void ratio with degree of saturation; (c) Vertical effective stress versus degree of saturation.

FIG. 8: (a) Sedimented Bonny silt SWRC data from this study along with the fitted van Genuchten (1980) SWRC model; (b) Comparison of the van Genuchten (1980) SWRC models for sedimented and compacted Bonny silt specimens.

FIG. 9: Evolution in yield stress for unsaturated sedimented and compacted Bonny silt specimens: (a) Yield stress as a function of degree of saturation at yielding; (b) Yield stress as a function of matric suction at yielding

FIG. 10: Evolution in suction stress as a function of matric suction at yielding for sedimented and compacted Bonny silt specimens.

FIG. 11: Evolution in the compression index with matric suction for sedimented and compacted Bonny silt specimens.

Figure 1

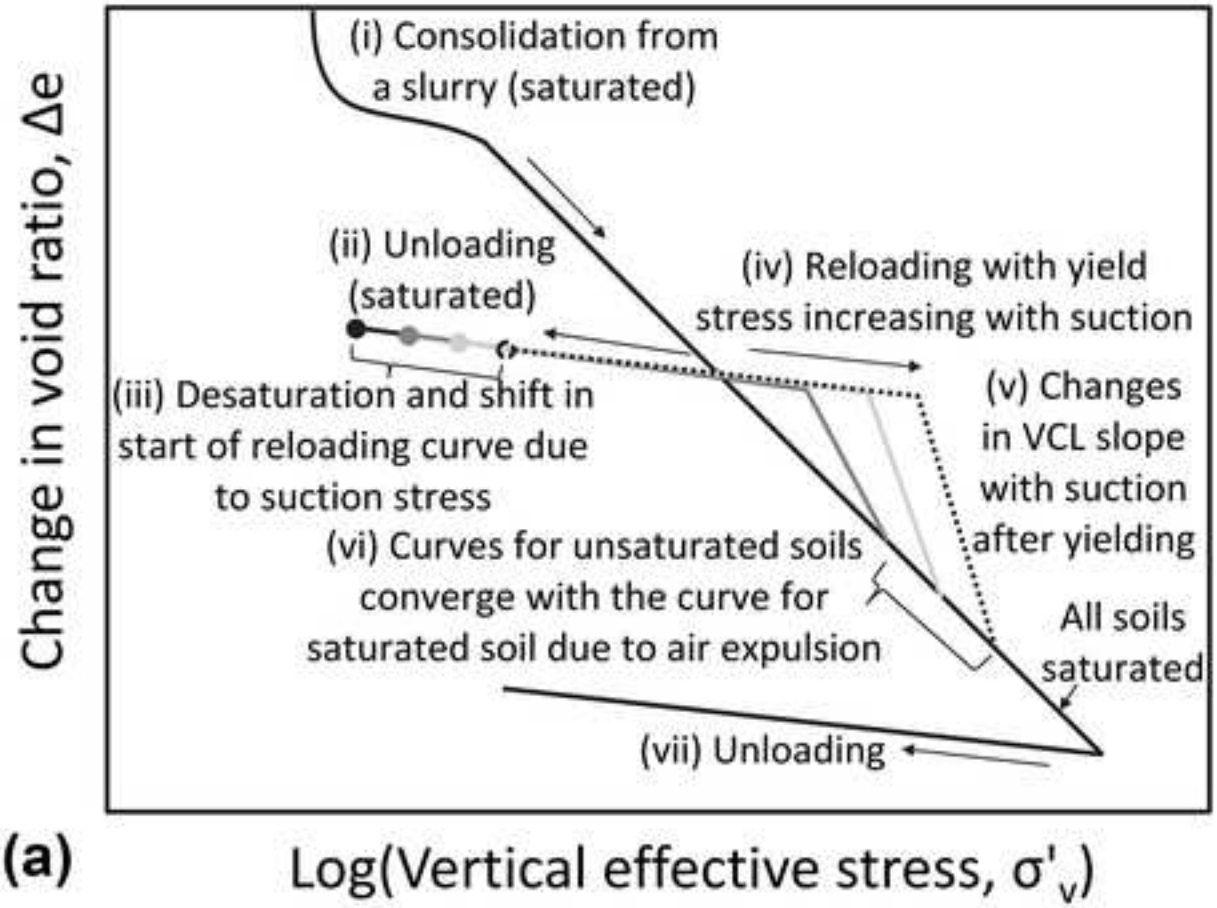

Change in void ratio, Δe
(i) Consolidation from a slurry (saturated)
(ii) Unloading (saturated)
(iii) Desaturation and shift in start of reloading curve due to suction stress
(iv) Reloading with yield stress increasing with suction
(v) Changes in VCL slope with suction after yielding
(vi) Curves for unsaturated soils converge with the curve for saturated soil due to air expulsion
All soils saturated
(vii) Unloading
Log(Vertical effective stress, σ'v)

(a)

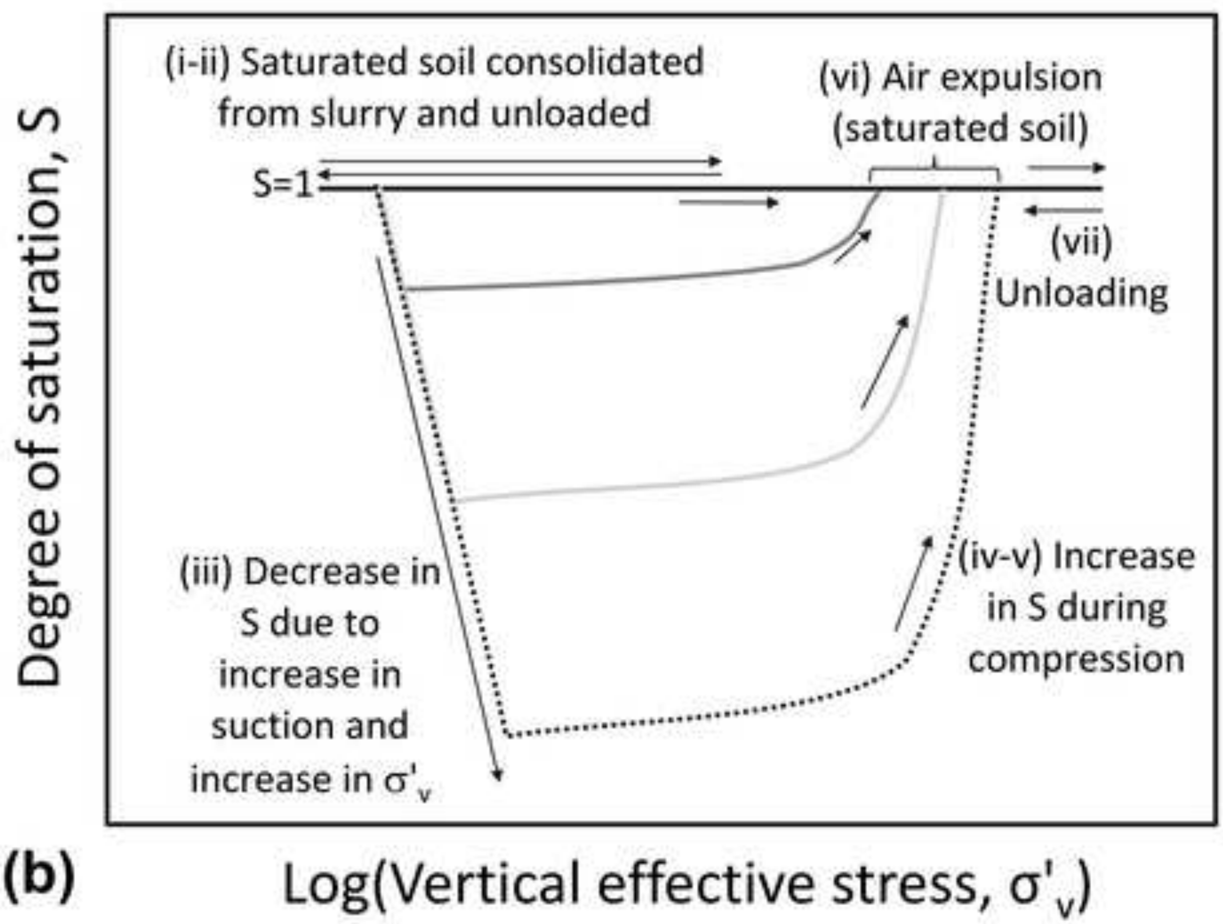

Degree of saturation, S
(i-ii) Saturated soil consolidated from slurry and unloaded
(vi) Air expulsion (saturated soil)
S=1
(vii) Unloading
(iii) Decrease in S due to increase in suction and increase in σ'v
(iv-v) Increase in S during compression
Log(Vertical effective stress, σ'v)

(b)

Figure 2

Click here to access/download;Figure;Figure 2.tif

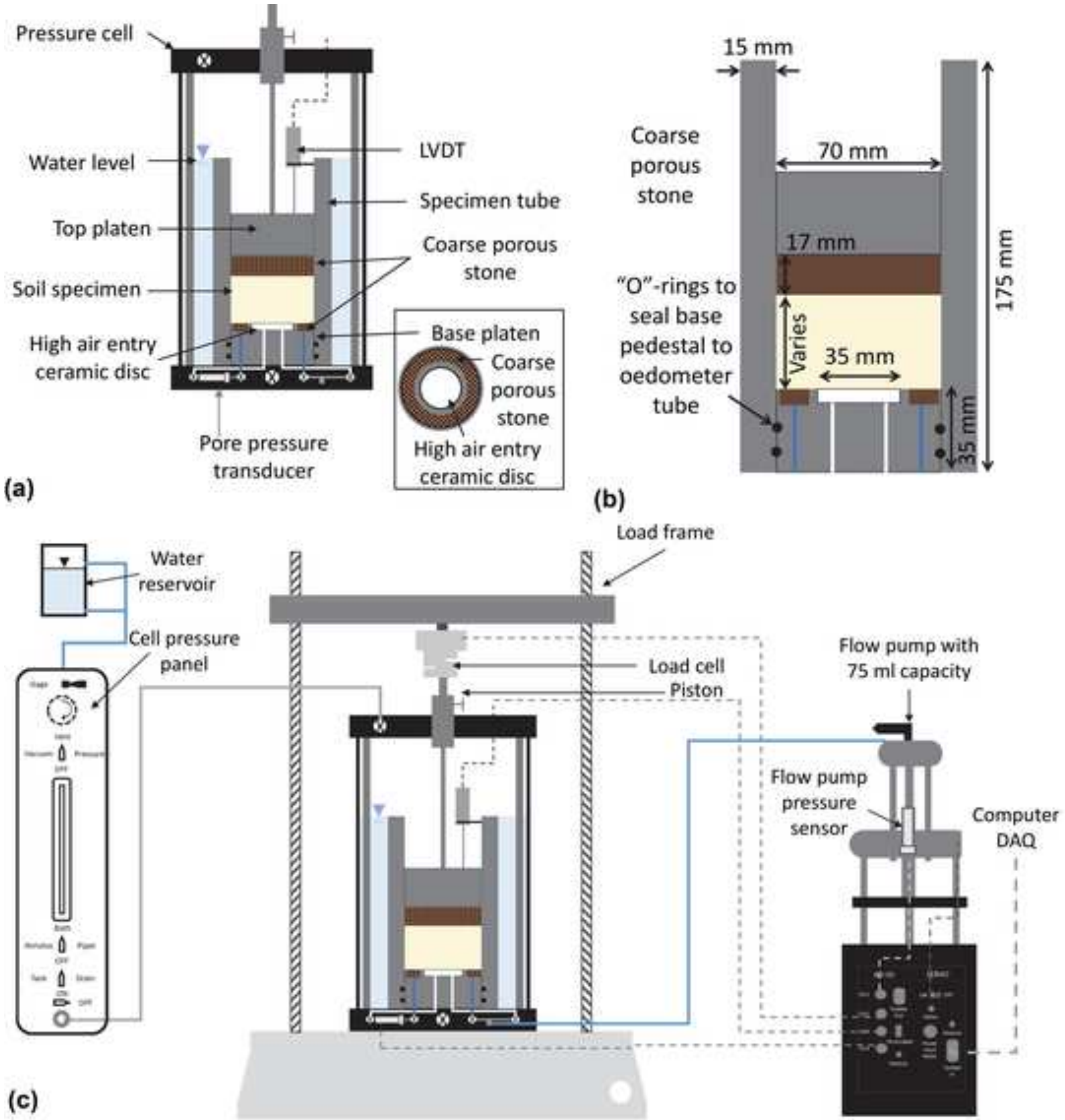

Figure 3

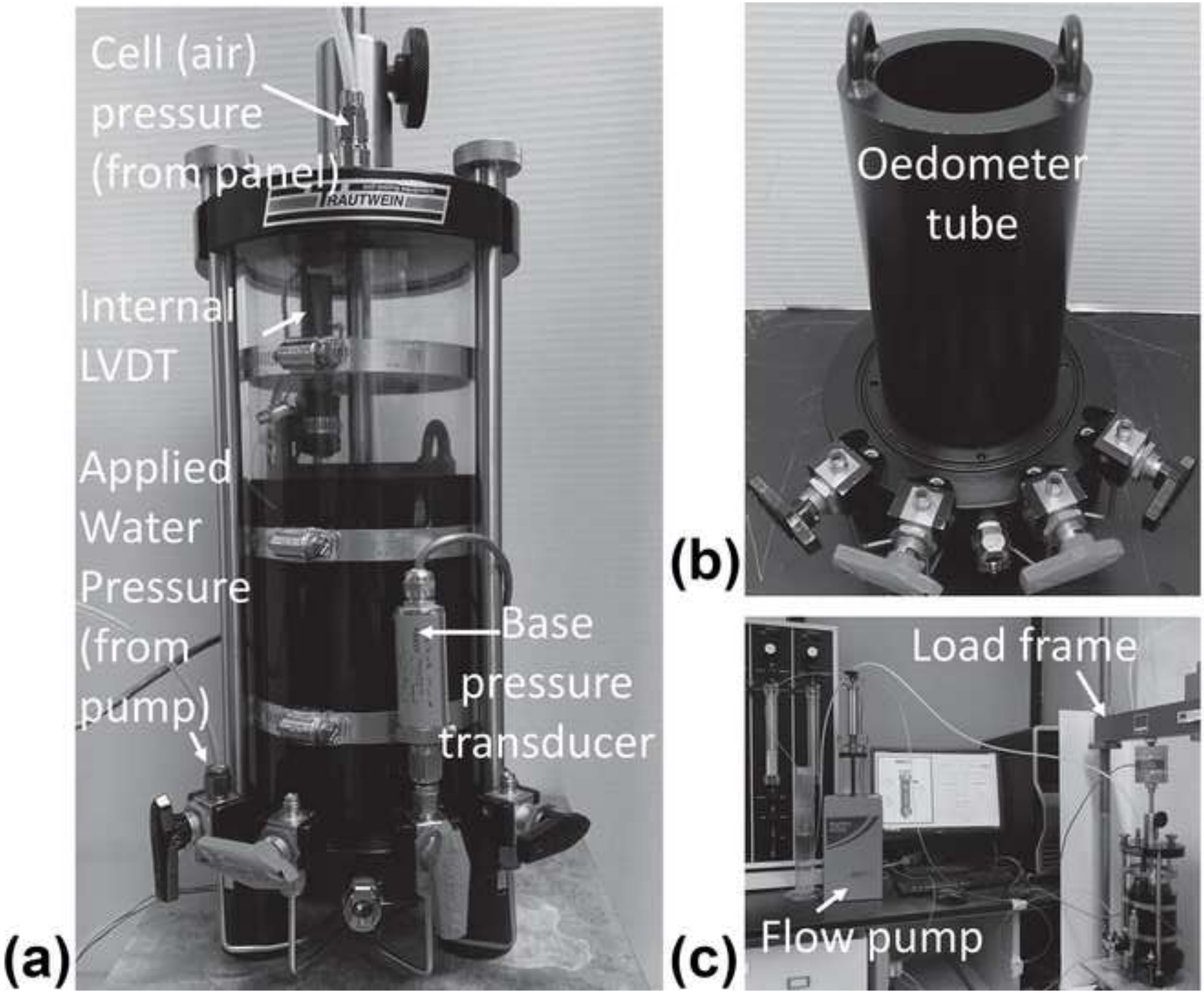
Cell (air) pressure (from panel)
RAUTWEIN
Internal LVDT
Applied Water Pressure (from pump)
Base pressure transducer
(a)
Oedometer tube
(b)
Load frame
Flow pump
(c)

Figure 4

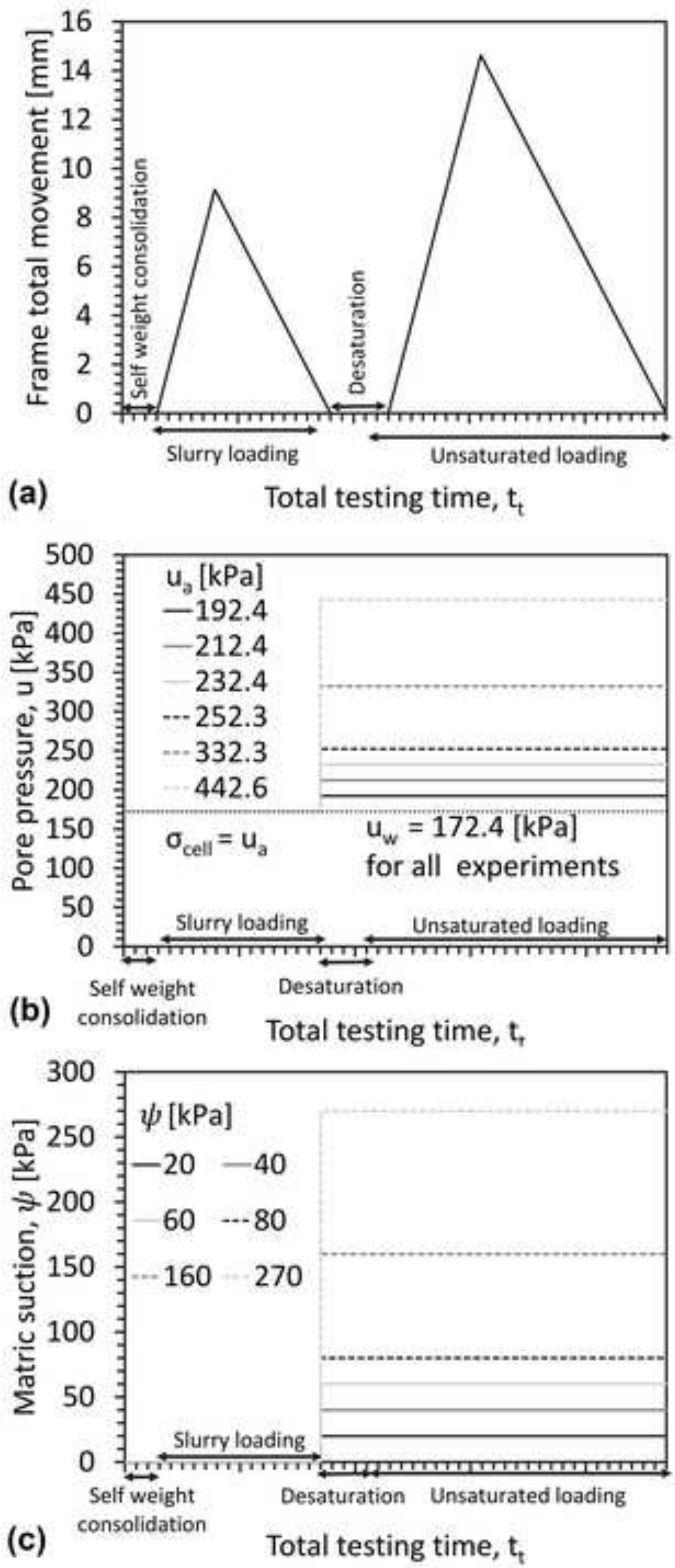

Frame total movement [mm]
16
14
12
10
8
6
4
2
0
Self weight consolidation
Desaturation
Slurry loading
Unsaturated loading
(a)
Total testing time, t_t
Pore pressure, u [kPa]
500
450
400
350
300
250
200
150
100
50
0
u_a [kPa]
192.4
212.4
232.4
252.3
332.3
442.6
$\sigma_{cell} = u_a$
u_w = 172.4 [kPa]
for all experiments
Slurry loading
Unsaturated loading
Self weight
consolidation
Desaturation
(b)
Total testing time, t_t
Matric suction, ψ [kPa]
300
250
200
150
100
50
0
ψ [kPa]
20
40
60
80
160
270
Slurry loading
Self weight
consolidation
Desaturation
Unsaturated loading
(c)
Total testing time, t_t

Figure 5

Click here to access/download;Figure;Figure 5.tif

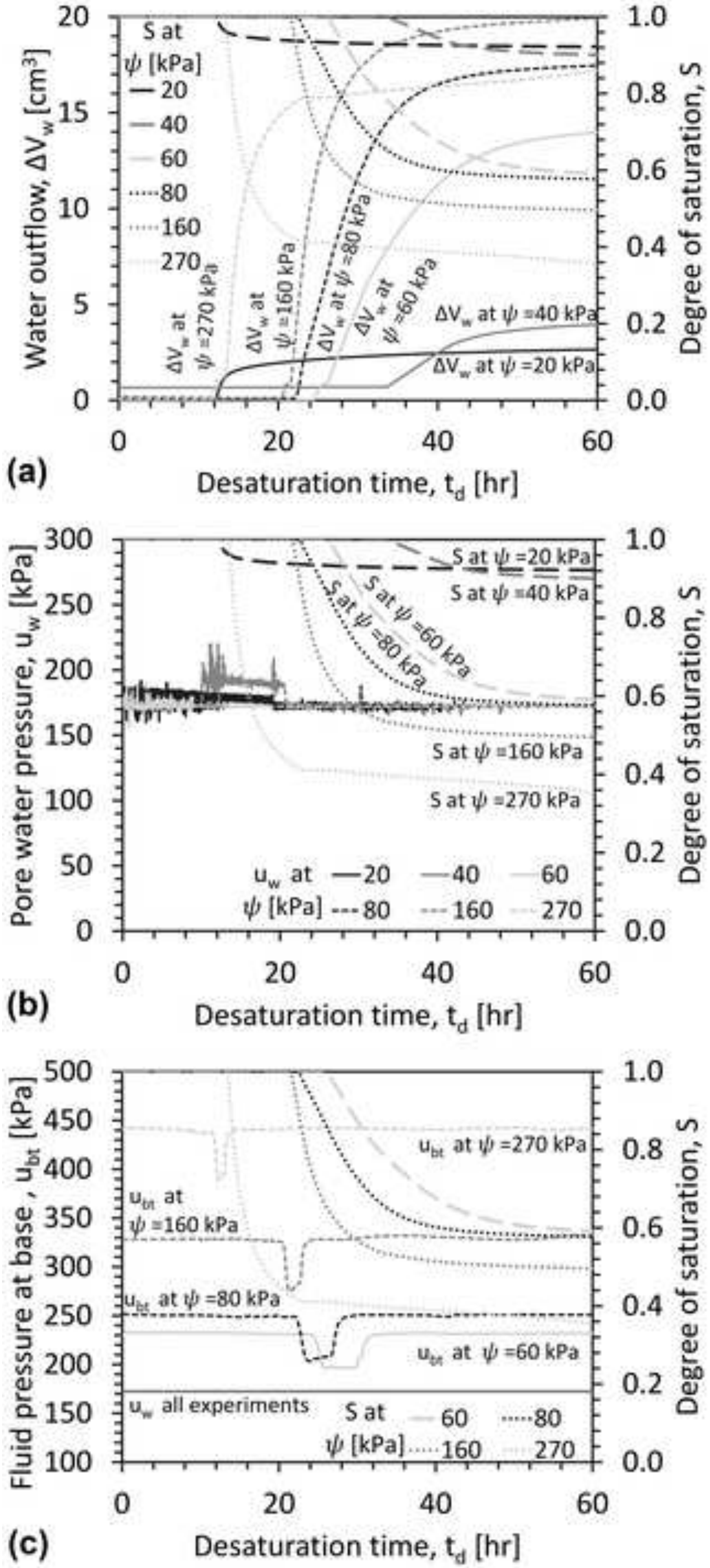

Figure 6

Click here to access/download;Figure;Figure 6.tif

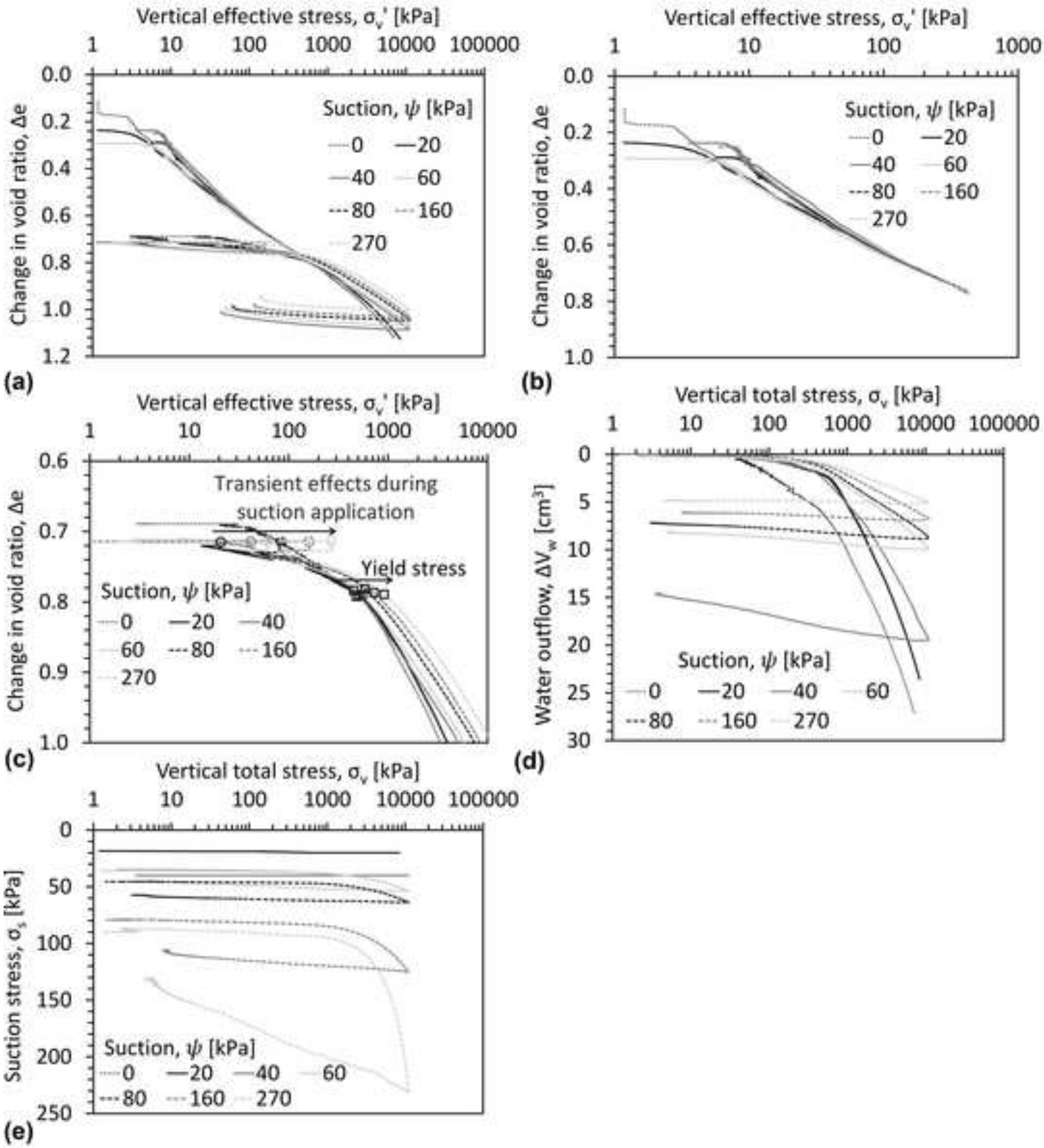

Figure 7

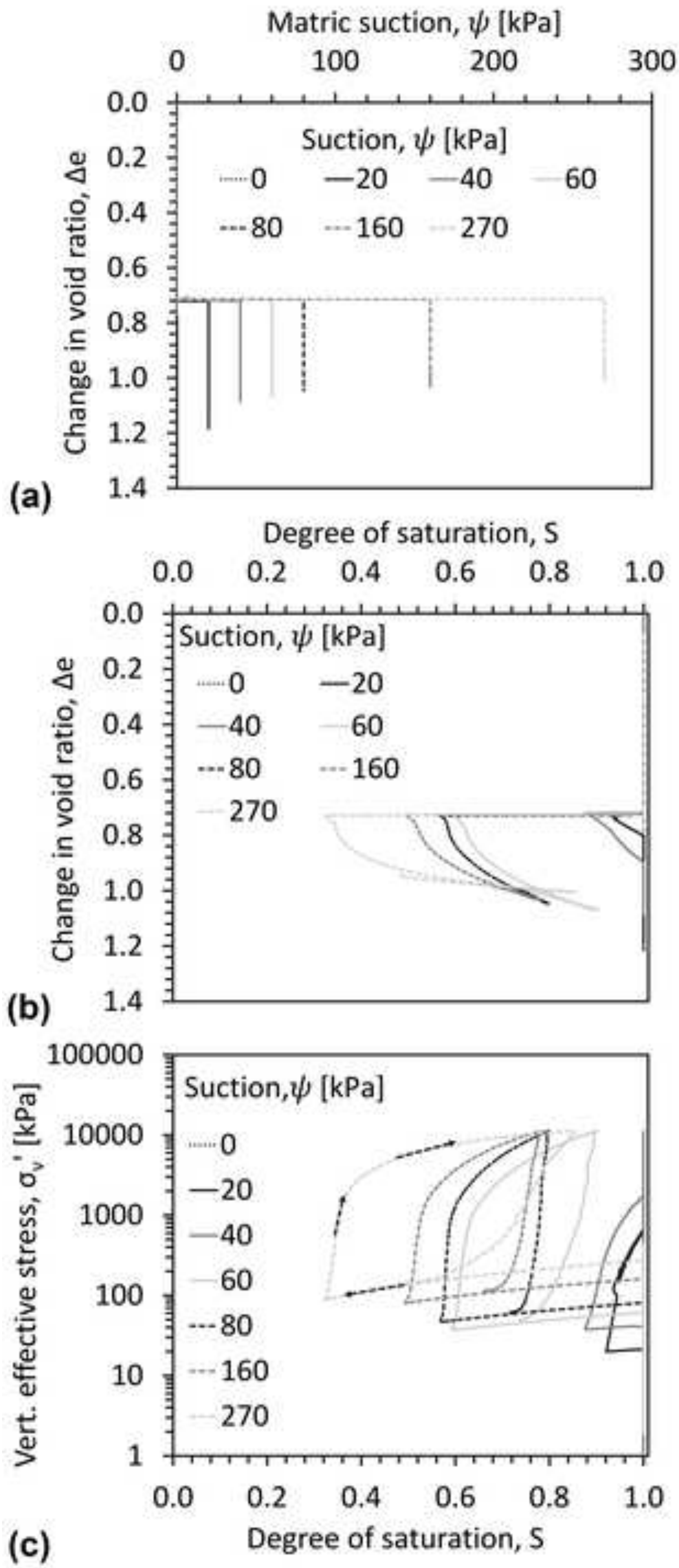

Matric suction, ψ [kPa]
0
100
200
300
Change in void ratio, Δe
0.0
0.2
0.4
0.6
0.8
1.0
1.2
1.4
Suction, ψ [kPa]
0
20
40
60
80
160
270
(a)
Degree of saturation, S
0.0
0.2
0.4
0.6
0.8
1.0
Change in void ratio, Δe
Suction, ψ [kPa]
(b)
100000
10000
1000
100
10
1
Vert. effective stress, σv' [kPa]
Suction,ψ [kPa]
Degree of saturation, S
(c)

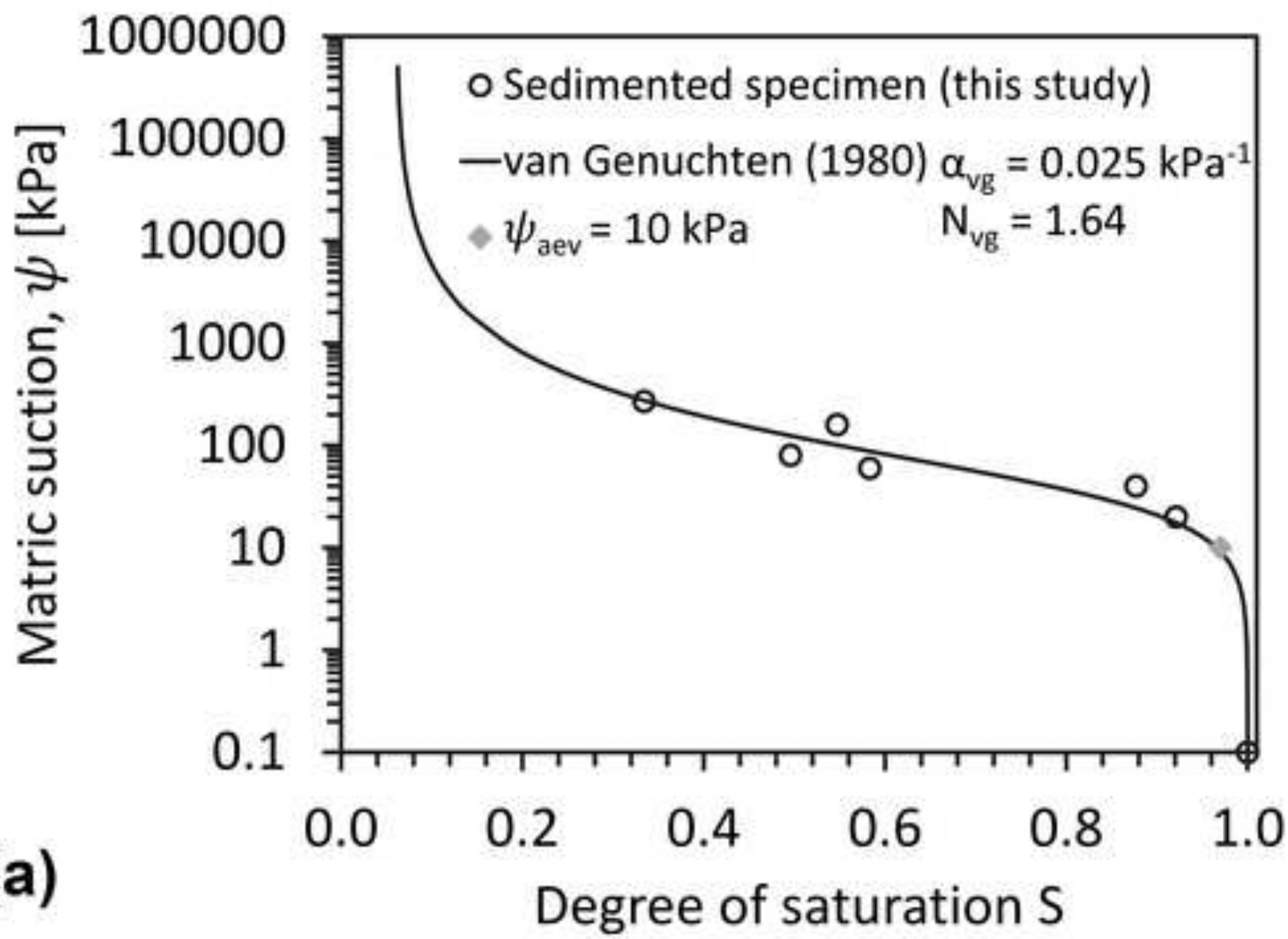

1000000
100000
10000
1000
100
10
1
0.1
Matric suction, ψ [kPa]
Sedimented specimen (this study)
van Genuchten (1980) α_{vg} = 0.025 kPa^{-1}
N_{vg} = 1.64
ψ_{aev} = 10 kPa
0.0
0.2
0.4
0.6
0.8
1.0
Degree of saturation S

(a)

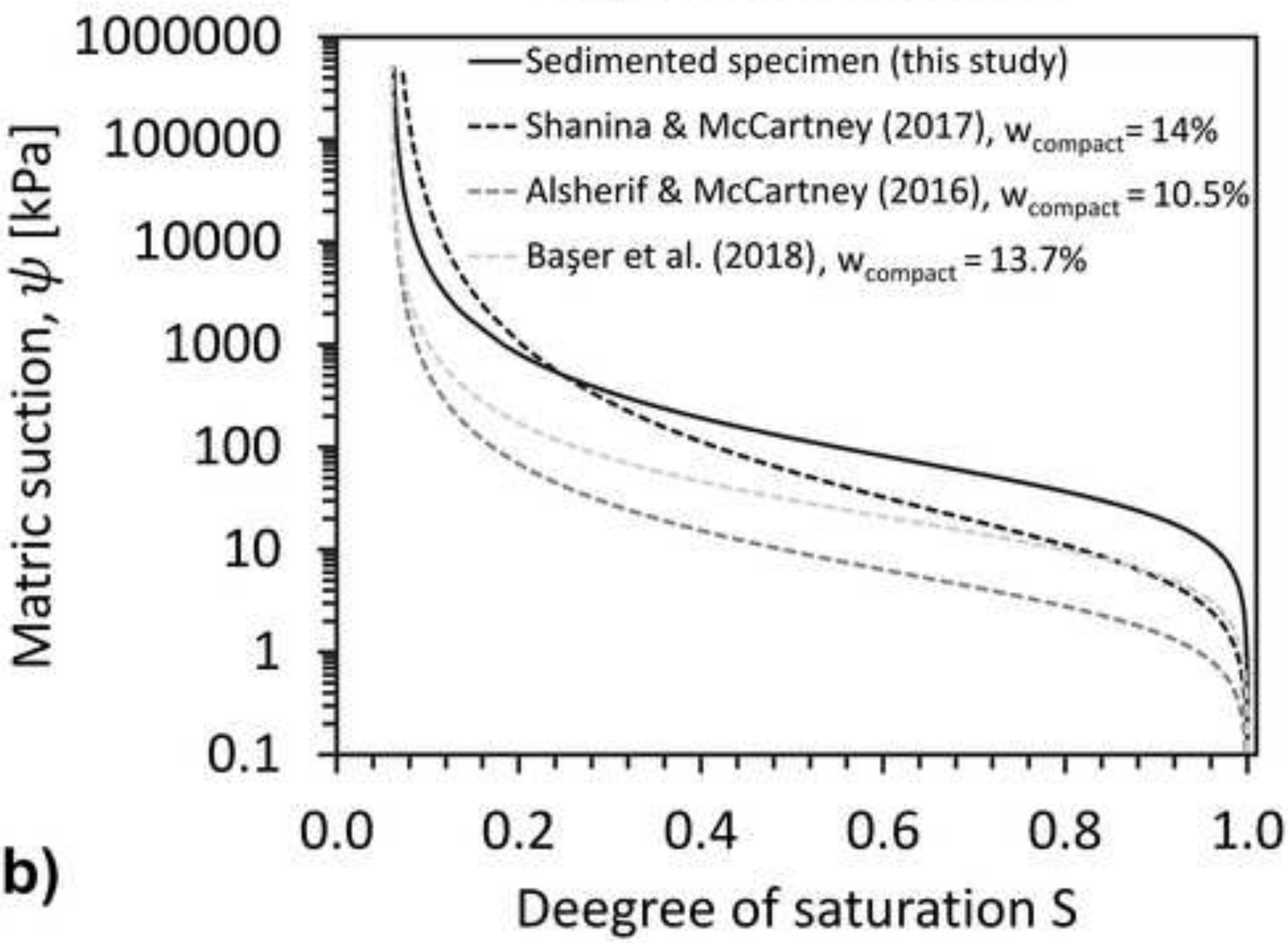

1000000
100000
10000
1000
100
10
1
0.1
Matric suction, ψ [kPa]
Sedimented specimen (this study)
Shanina & McCartney (2017), $w_{compact}$ = 14%
Alsherif & McCartney (2016), $w_{compact}$ = 10.5%
Başer et al. (2018), $w_{compact}$ = 13.7%
0.0
0.2
0.4
0.6
0.8
1.0
Deegree of saturation S

(b)

Figure 9

Click here to access/download;Figure;Figure 9.tif

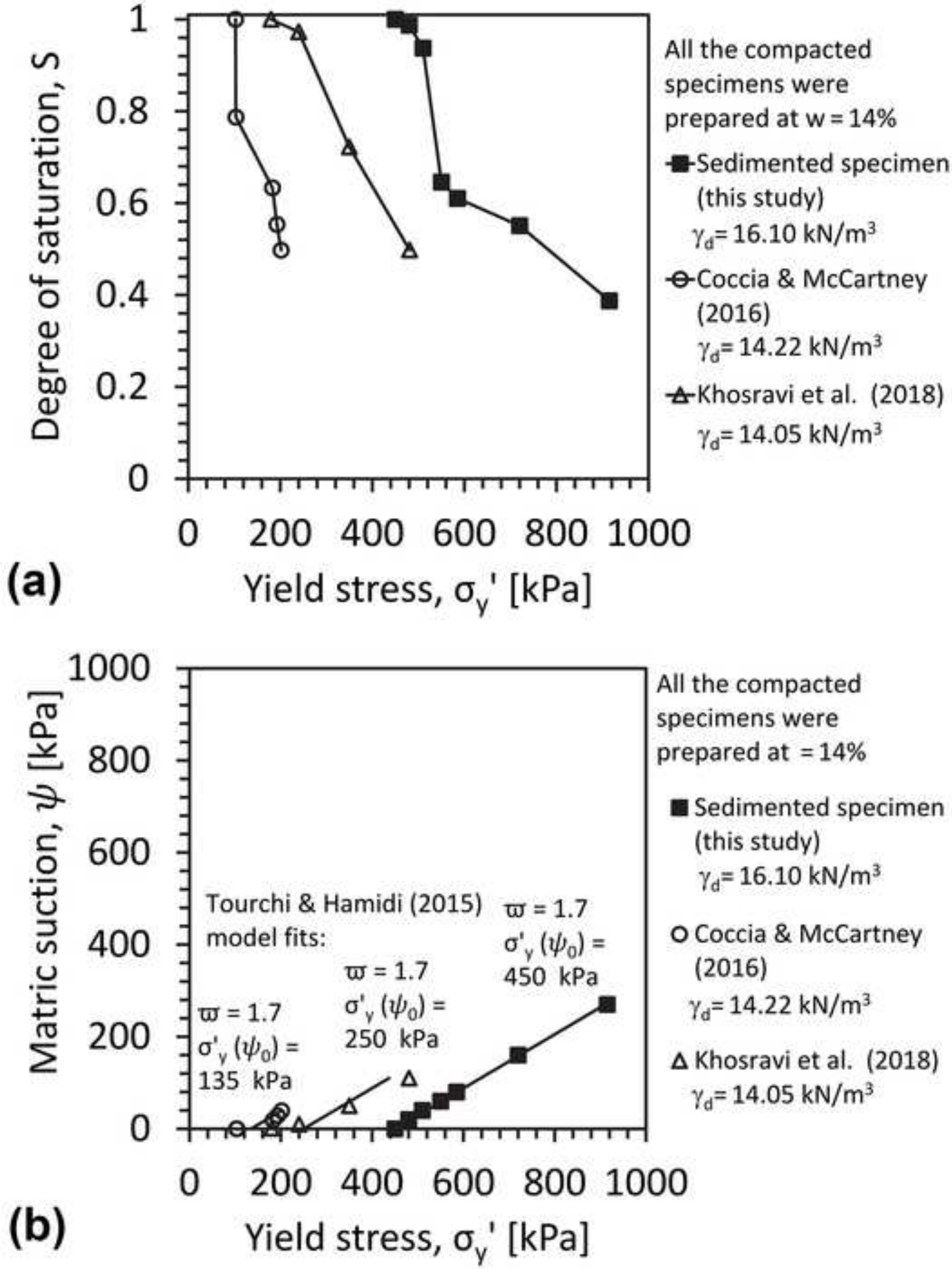

Figure 10

Click here to access/download;Figure;Figure 10.tif

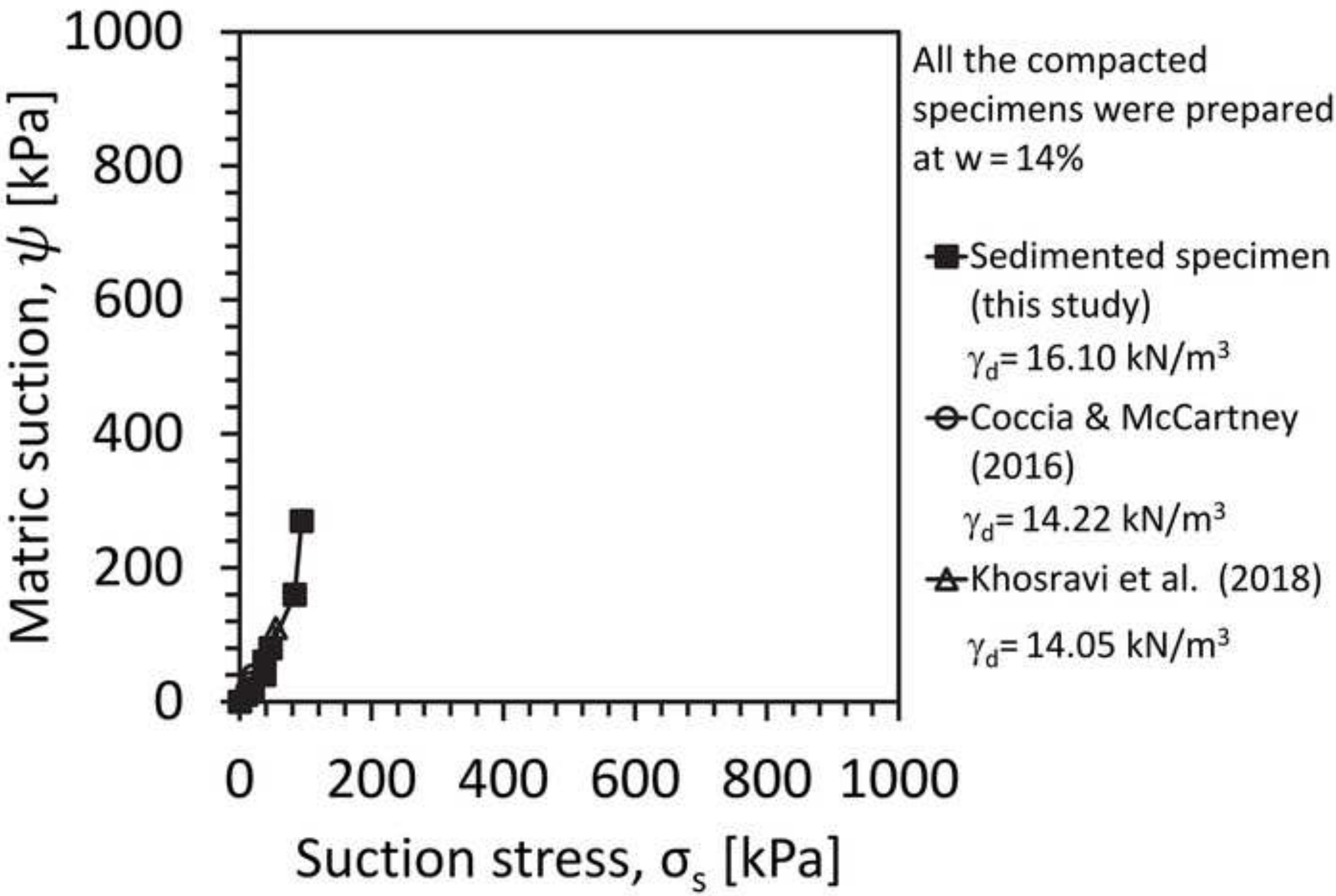

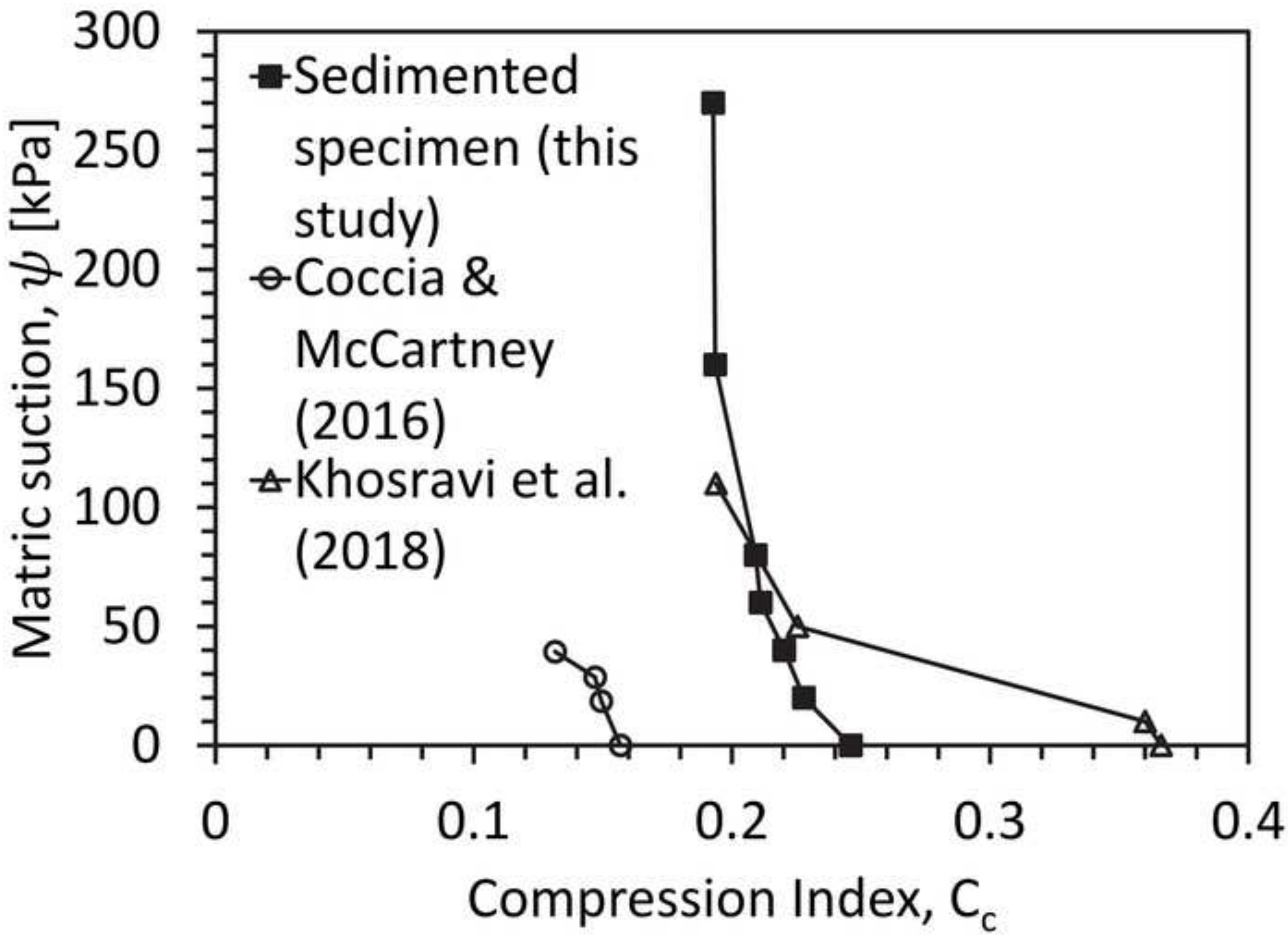
300
250
200
150
100
50
0
0
0.1
0.2
0.3
0.4
Matric suction, ψ [kPa]
Compression Index, C_c
Sedimented specimen (this study)
Coccia & McCartney (2016)
Khosravi et al. (2018)